

Structural, electronic, and effective-mass properties of silicon and zinc-blende group-III nitride semiconductor compounds

L. E. Ramos,¹ L. K. Teles,¹ L. M. R. Scolfaro,¹ J. L. P. Castineira,² A. L. Rosa,¹ and J. R. Leite¹

¹Universidade de São Paulo, Instituto de Física, Caixa Postal 66318, 05315-970 São Paulo, SP, Brazil

²Universidade Federal de Uberlândia, Departamento de Ciências Físicas, Caixa Postal 593, 38400-902 Uberlândia, MG, Brazil

(Received 12 June 2000; revised manuscript received 16 October 2000; published 5 April 2001)

The electronic band structures of silicon and the zinc-blende-type III-N semiconductor compounds BN, AlN, GaN, and InN are calculated by using the self-consistent full potential linear augmented plane wave method within the local-density functional approximation. Lattice constant, bulk modulus, and cohesive energy are obtained from full relativistic total-energy calculations for Si and for the nitrides. Band structures and total density of states (DOS) are presented. The role played by relativistic effects on the bulk band structures and DOS is discussed. In order to provide important band structure-derived properties, such as effective masses and Luttinger parameters, the *ab initio* band structure results are linked with effective-mass theory. Electron, heavy-, light-, and split-off-hole effective masses, as well as spin-orbit splitting energies are extracted from the band-structure calculations. By using the Luttinger-Kohn 6×6 effective-mass Hamiltonian we derive the corresponding Luttinger parameters for the materials. A comparison with other available theoretical results and experimental data is made.

DOI: 10.1103/PhysRevB.63.165210

PACS number(s): 71.20.Nr, 71.18.+y, 71.70.Ej

I. INTRODUCTION

The production of highly efficient blue and green light-emitting diodes and the development of laser diodes operating in the blue-ultraviolet spectral regions have stimulated intensive studies of group-III nitride semiconductor materials.^{1,2} The nitrides exhibit several interesting properties, such as wide band gaps, high thermal conductivities, and hardness, which make them also useful for device applications at high pressures and temperatures.^{3,4} Group-III nitride-based heterostructures have been grown using both hexagonal (wurtzite) and cubic (zinc-blende) crystals. The wurtzite phase of the III-N compounds constitutes the thermodynamically most stable configuration (with the exception of BN). Recently, with the significant progress in crystal growth and material processing technologies, AlN,⁵ GaN,⁶⁻¹⁰ InN,¹¹ InGaN,¹² and AlGaN (Ref. 13) epitaxial layers of cubic, zinc-blende (ZB)-type have successfully been grown. According to the general trends of the material properties of III-V compound semiconductors, the metastable cubic (c-) phase offers technological advantages compared to its wurtzite (w-) one, such as the ability to produce cleaved laser cavities and the ease to perform a controlled doping.⁴ Moreover, the common acceptor and donor levels seem to appear with smaller ionization energies with respect to the band edges of the cubic materials. BN, the lightest of the III-N compounds, is unique among the nitrides, which is more stable in the ZB structure.

The already observed progress in the production of thin films of group-III nitrides has stimulated a great deal of theoretical investigations aiming a deeper understanding of their bulk electronic and structural properties. Not only GaN, AlN, or InN epitaxial layers and their alloys have potential for applications, but so do BN, BAlN, and BGaN layers.^{3,14,15} On the other hand, the practical interest in realizing, e.g., ZB-based GaN/AlGaN, and InGaN/GaN quantum wells for fu-

ture wide-energy band-gap device concepts faces the need of reliable information also on band structure-derived quantities such as effective masses and/or Luttinger parameters. The lack of these informations, particularly for the c-phase of the compounds has been recently raised by us.¹⁶

Some theoretical attempts to provide effective-mass parameters of III-N's have been carried out for c-GaN and AlN, and w-GaN and InN through empirical pseudopotential calculations,^{17,18} and for w-AlN and w- and c-GaN by using the *ab initio* full potential linear augmented plane wave (FLAPW) method.^{19,20} The inclusion of spin-orbit interaction effects in the bulk band-structure calculations has been considered in various works,^{17-19,21,22} although in some of them these effects are taken into account through empirical parameters adjusted to give the values obtained from first-principles calculations.^{17,18,23,24} Due to the fact that the spin-orbit interaction and other relativistic effects, i.e., Darwin and mass-velocity corrections, are important in the description of the nitride electronic properties, particularly for those involving the heavier elements Ga and In, we analyze the role played by these effects also in the band structure. For BN, there are no reports on effective masses and Luttinger parameters, so far.

In this paper, our aim is to present a systematic study of the structural and electronic properties of Si and of c-BN, AlN, GaN, and InN by using the *ab initio* self-consistent FLAPW within the local-density functional (LDF) approach, and to derive conduction- and valence-band effective masses, as well as the Luttinger parameters. Although there already exist several reports on effective-mass parameters from independent groups in the literature, they are obtained from different methods and/or only for some of the compounds. Thus, a detailed and consistent calculation of these parameters for the whole series of nitrides will be very useful and welcome.

We performed band-structure calculations for all the ni-

TABLE I. Lattice constant (in Å) of cubic BN, AlN, GaN, and InN.

	BN	AlN	GaN	InN
Expt.	3.616 ^a	4.38 ^{a,c}	4.50 ^b	4.98, ^d 4.97 ^e
This work	3.63	4.40	4.552	5.03
Other calc.	3.59, ^f 3.615, ^g 3.62 ^h	4.32, ^f 4.342, ⁱ 4.36, ^h 4.394, ^j 4.345 ^k	4.46, ^{f,i} 4.43, ^h 4.59, ^j 4.464 ^k	4.92, ^{f,h} 4.932, ⁱ 4.957, ^k 5.109 ^j

^aReference 4.^bReference 35.^cReference 36.^dReference 37.^eReference 11.^fFLMTO within LDA from Ref. 38.^gOrthogonalized LCAO within LDA from Ref. 39.^hLMTO-ASA within LDA from Ref. 40.ⁱPWPP within LDA from Ref. 41.^jPWPP within GGA from Ref. 22.^kFLMTO within LDA from Ref. 42.

trides, providing first accurate values for the lattice constants, bulk moduli, and cohesive energies that can also be compared with the available experimental data. Band structures and total density of states are also shown. Through the obtained dispersion relations along the high symmetry directions of the Brillouin zone (BZ), and focusing on the valence-band maximum and the conduction-band minimum at Γ (or at the \mathbf{k} point corresponding to the absolute conduction-band minimum for the indirect gap materials), we link the electronic band-structure calculation with the effective-mass theory. For the valence-band fitting, a 6×6 Luttinger-Kohn Hamiltonian was used.²⁵ Owing to the fact that the conduction-band minimum at Γ is a nondegenerate band, we adopted a parabolic model to derive electron masses. For BN and AlN, as well as for Si, since the conduction-band minimum does not occur at the Γ point, transversal and longitudinal electron effective masses are properly derived.

As silicon is a well-known semiconductor material, widely investigated from both the experimental and theoretical points of view, and due to the fact that Si constitutes an “intermediate” material example (i.e., between the nitrides and GaAs, the most studied compound among the III-V’s), concerning the importance of spin-orbit coupling effects, we also carried out calculations of the band structure of Si, as a prototype, evaluating its conduction- and valence-band effective masses and corresponding Luttinger parameters.

The paper is organized as follows. In Sec. II we describe the *ab initio* FLAPW band-structure calculations and present the results for the structural and electronic properties. In Sec. III the 6×6 Luttinger-Kohn model used in the fitting of the valence-band structures close to the Γ point is briefly described. The results obtained for the effective masses and Luttinger parameters are also shown in this section. In Sec. IV we draw the conclusions.

II. AB INITIO FLAPW CALCULATIONS: BAND-STRUCTURE RESULTS

The structural and electronic properties of Si and of the c-BN, AlN, GaN, and InN were obtained by means of *ab initio* all electron self-consistent electronic structure calculations through the FLAPW method.^{26,27} The local-density

functional theory is used. The electron gas data for the exchange-correlation potential were taken from Perdew, Burke, and Ernzerhof, the so-called generalized gradient approximation (GGA),²⁸ unless mentioned otherwise. The B $2s$, $2p$, the N $2s$, $2p$, the Al $3s$, $3p$, the Ga $3p$, $3d$, $4s$, $4p$, and the In $4p$, $4d$, $5s$, and $5p$ electrons were treated as part of the valence-band states. Particularly, the Ga $3d$ and In $4d$ orbitals are known to play an important role in the correct description of the energy bands since they hybridize strongly with N- $2s$ states.^{19–21} The inclusion of the Ga- $3p$ and In- $4p$ orbitals, among the valence states, ensured that no charge is left out of the atomic spheres. The separation energy between core and valence states was chosen differently in each compound in order to guarantee this condition. The cutoff angular momentum was $l=10$ for wave functions and $l=5$ for charge densities and potentials inside the spheres. Equal values were assumed for the muffin-tin sphere radii of both atoms in each material, $1.46 a_B$ for BN, $1.8 a_B$ for AlN and GaN, $1.9 a_B$ for InN and Si, where a_B is the free electron Bohr radius. The number of \mathbf{k} points used as input for the determination of the self-consistent charge density was 343, which corresponded to 30 \mathbf{k} points in the irreducible symmetry wedge of the BZ. With these assumptions, the self-consistent energy bands were converged within 10^{-5} eV and the total energy within 10^{-6} eV. The core electron states were treated full relativistically, whereas the valence states were treated both nonrelativistic and semirelativistically, i.e., within a scalar-relativistic treatment²⁹ or via a second variational method including spin-orbit coupling.³⁰ In our full relativistic calculations we perform first a self-consistent calculation converging the total energy within the scalar-relativistic approximation. Then, by using the converged potential, we perform a second self-consistent calculation including the spin-orbit term and converging the total energy again.

A. Structural properties

The calculated total energies and pressures for several lattice constants were fitted with the empirical Murnaghan equation of state³¹ to obtain equilibrium lattice constants and bulk moduli. Table I shows the obtained lattice constant a for all the ZB nitrides, whereas the values obtained for the bulk

TABLE II. Bulk modulus (in GPa) for cubic BN, AlN, GaN, and InN.

	BN	AlN	GaN	InN
Expt.	290–465 ^a	207.9±6.3 ^b	237±31 ^b	125.5±4.6 ^b
This work	386	198	192	138
Other calc.	392–400, ^c 370, ^d 378 ^f	191, ^e 203, ^c 215, ^f 207 ^g	156, ^e 184, ^f 187, ^g 201 ^{c,h}	117, ^e 137, ^f 139 ^{c,h}

^aReference 4.^bReference 43—values for the wurtzite phase.^cReference 38.^dReference 39.^eReference 22.^fReference 40.^gReference 41.^hReference 42.

modulus B are depicted in Table II. These results are compared with the experimental data and previous calculations. The values for a are in very good agreement with the measured values and with recent theoretical results obtained from rigorous plane-wave pseudopotential (PWPP) and full potential linear muffin-tin orbital (FLMTO) calculations. The predicted theoretical values for the lattice constants are about 1% larger than the experimental ones. This is a consequence of the use of GGA in the treatment of exchange-correlation effects.³² If instead, the current local-density approximation (LDA) is used, the values of a are approximately 1–2% smaller than the experimental values. A detailed comparison between band-structure calculations for w- and c-AlN, GaN, and InN using LDA and GGA has recently been reported.²²

The values for the cohesive energy are displayed in Table III for the series of the group-III nitrides. The FLAPW code provides atomic energies within a full relativistic calculation.³³ This means that the total (bulk) and atomic energies are calculated in a different way, the former by perturbation theory. In order to have these quantities calculated in the same approximation, we applied a procedure suggested in Ref. 34. We calculated the total energy of a fcc lattice for Si, N, B, Al, Ga, and In, converging it with respect to the lattice constant whose value was chosen as large as possible. The total energy of such a lattice should correspond to the atomic energy calculated in the same approximation as the III-N's and Si. Although the results should be independent of the muffin-tin radii, we used the same values as for the binary compounds, except N, for which we have chosen $1.8 a_B$.

TABLE III. Cohesive energy per pair (in eV) for cubic BN, AlN, GaN, and InN. Values in parentheses correspond to those obtained from nonrelativistic calculations.

	BN	AlN	GaN	InN
Expt.	13.36 ^a	11.52 ^a	8.96 ^a	7.72 ^a
This work	17.39 (17.40)	14.81 (14.85)	12.01 (12.24)	10.39 (10.97)
Other calc.	14.3 ^d	11.36, ^e 10.88 ^f	8.25, ^e 8.35, ^f 10.64, ^b 12.00 ^c	6.85, ^e 6.99 ^f

^aReference 45 for the wurtzite phase.^bReference 46—Pseudopotential within LDA including GW corrections.^cFLAPW within LDA from Ref. 20.^dReference 47—*Ab initio* pseudopotential within LDA.^eReference 22—PWPP within GGA.^fReference 44—Self-consistent Hartree-Fock including configuration interaction.

We performed just a relativistic calculation, neglecting the spin-orbit interaction since this procedure showed not to affect much the total energy values. The separation energy between the core and valence states was fixed at –8.0 Ry in order to adopt a common energy value for all the calculations. In Table II we observe that the magnitude of B increases with the decrease of the cation mass confirming that BN is the hardest material, followed by AlN, GaN, and InN. The same behavior is observed for the cohesive energy, indicating that the B-N bond is stronger than Al-N and so on, which is also observed for the group-III arsenides.⁴⁸

Table IV supplies the values of a , B , and for the cohesive energy E_{coh} , as obtained for silicon. Excellent agreement with experiment and also with other theoretical results is observed for a (within less than 1%), and surprisingly good accordance between the calculated and measured values for the bulk modulus, since a measure of this is known to be difficult. The differences encountered between cohesive energies obtained from nonrelativistic and full relativistic calculations were less than 0.1 eV for Si, BN, and AlN, and of the order of 0.2 eV (1.6%) and 0.6 eV (5.7%) for GaN and InN, respectively.

B. Electronic Properties

For the theoretical value of the lattice parameter, we calculated the corresponding band structure along the main symmetry directions of the BZ. Figures 1–4 depict the band structures and total density of states (DOS) for the series of

TABLE IV. Lattice parameter, a (in Å), bulk modulus, B (in GPa), and cohesive energy per pair, E_{coh} (in eV) for Si.

Si	a	B	E_{coh}
Expt.	5.43 ^a	99 ^b	9.28 ^b
This work	5.47	89	10.80(10.84) ^e
Other calc.	5.45, ^c 5.42 ^d	95, ^c 115 ^d	10.8 ^d

^aReferences 48 and 51.

^bReference 45.

^cReference 49—FLAPW within LDA.

^dReference 50—EXX (exact exchange method).

^eIn parenthesis the value from a nonrelativistic calculation.

nitrides. We show results obtained from nonrelativistic calculations in comparison to relativistic ones, the latter including spin-orbit interaction. The minimum energy gap was found at the Γ point for InN and GaN, at the X -point for AlN and BN, and at 85% of the Γ X line (near X point) for Si. The band structure and the total DOS for Si are shown in Fig. 5. The band-gap widths are underestimated, as a consequence of the LDF approximation. Particularly for InN, a negative value (-0.48 eV with a full relativistic calculation) for the band gap was found. Table V shows the calculated fundamental band-gap energies, as well as valence-band widths in

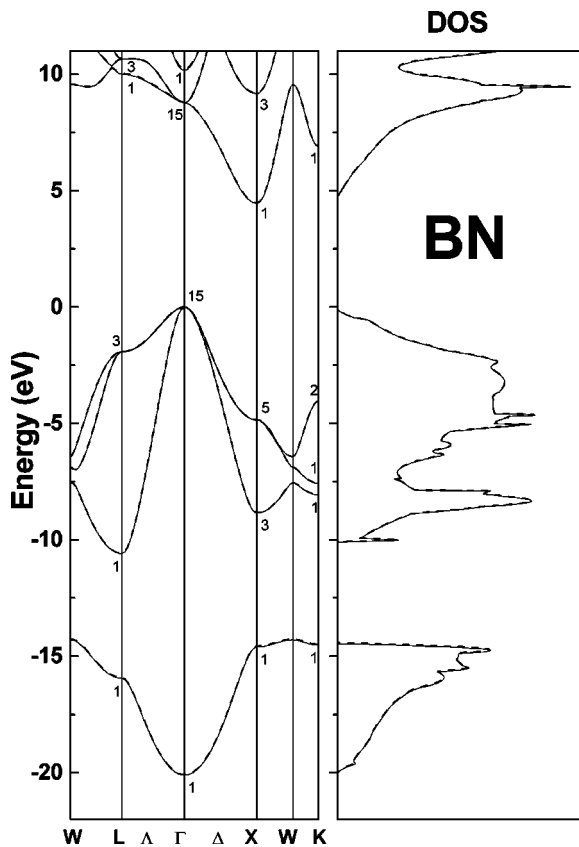


FIG. 1. Band structure and total DOS of zinc-blende BN. The zero of energy was placed at the top of the valence band. Full relativistic calculations (solid line); nonrelativistic calculations (dashed line). The labels of the energy levels are ascribed according to the single symmetry point group of the crystal.

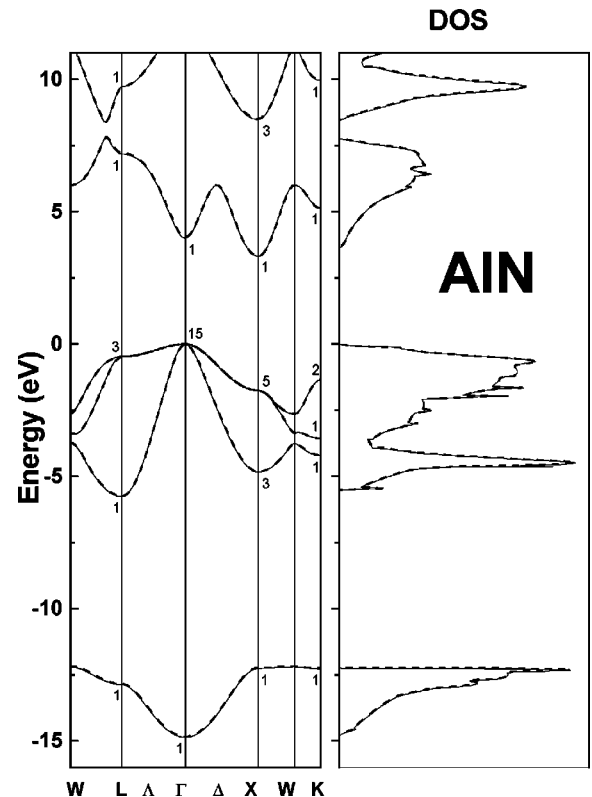


FIG. 2. Band structure and total DOS of zinc-blende AlN. The zero of energy, meaning of the lines, and labels ascribed to the levels are according to Fig. 1.

the series of nitrides, comparing results obtained without and with relativistic effects taken into account. While for BN and AlN the relativistic effects are responsible for changes in the band-gap energies by less than 1%, for GaN and InN, the inclusion of relativistic corrections are increasingly more important. *Ab initio* calculations for InN that include also self-interaction energy corrections or a more exact treatment of exchange effects have shown to improve the results for gap energies, although they are still far from the experimental value.^{52,53} The trend in the valence-band widths is affected by the dispersion of the $3d$ (Ga)- and $4d$ (In)-orbitals derived states, which lie close to the bottom of the valence band. As expected from a simple atomic energy picture, the d - s mixture is stronger for InN giving rise to a larger band dispersion at the valence-band bottom. These overall findings are consistent with several band-structure calculations reported previously.^{19–22,34,55,56}

Due to the spin-orbit interaction, we can see a spin-orbit-splitting energy Δ_{so} of the Γ_{15} state at the valence-band maximum into fourfold degenerate Γ_8 and twofold degenerate Γ_7 states. Table VI shows the calculated results and measured values, when available, of spin-orbit splitting energies, Δ_{so} . The calculated values of Δ_{so} for AlN are as small as those for GaN. In general, the magnitude of the spin-orbit coupling is not sensitive to the structural parameters, and it increases with atomic number.⁴⁸ Since in group-III nitrides, the top of the valence band is originated mainly from p -orbitals of nitrogen, with a small mixture of d character, Δ_{so} is very small compared to other III-V compounds. The

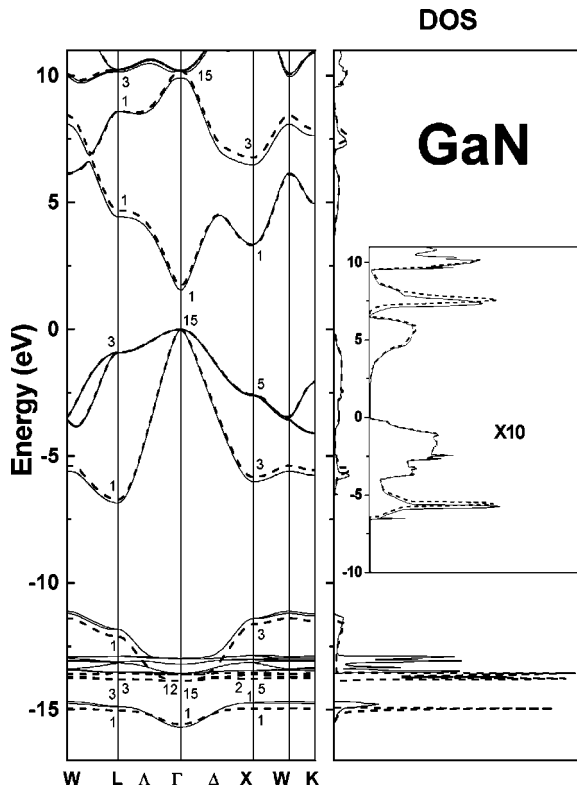


FIG. 3. Band structure and total DOS of zinc-blende GaN. The zero of energy, meaning of the lines, and labels ascribed to the levels are according to Fig. 1.

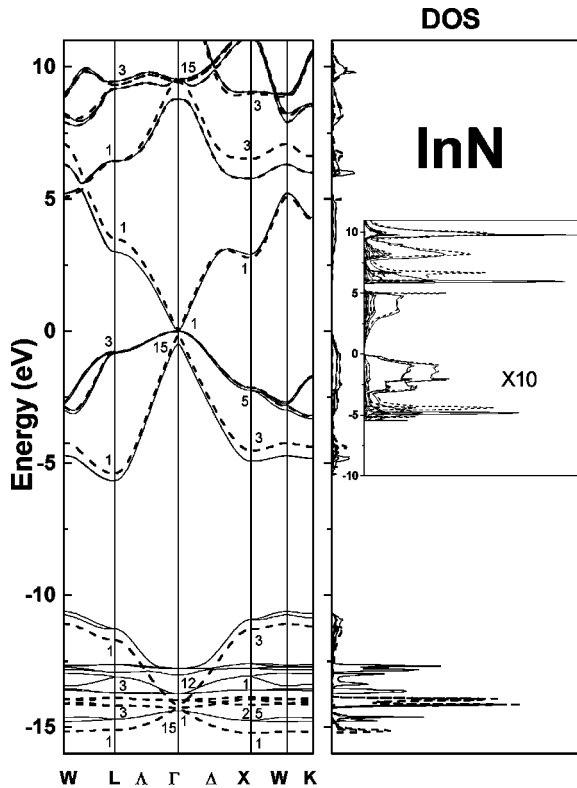


FIG. 4. Band structure and total DOS of zinc-blende InN. The zero of energy, meaning of the lines, and labels ascribed to the levels are according to Fig. 1.

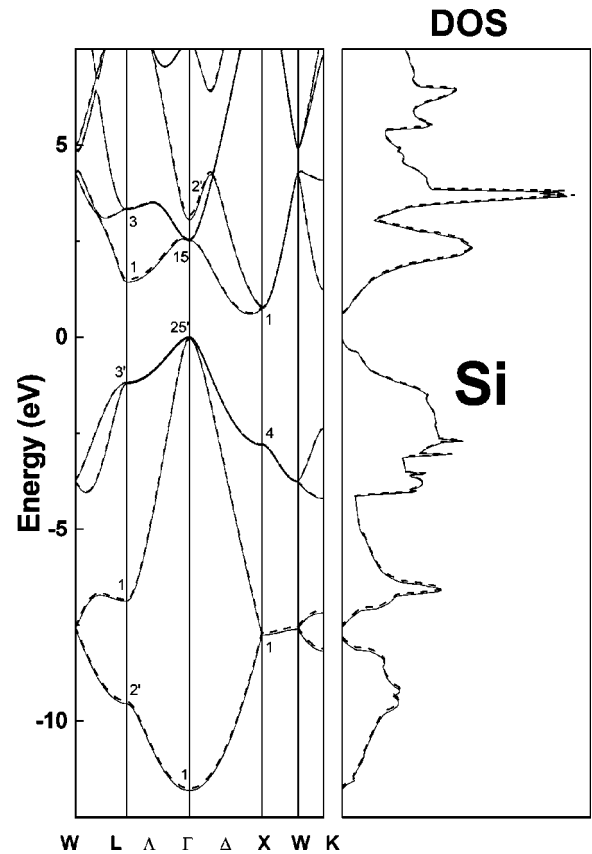


FIG. 5. Band structure and total DOS of Si. The zero of energy, meaning of the lines, and labels ascribed to the levels are according to Fig. 1.

same trend has been predicted by previous LAPW-LDA calculations performed on AlN, GaN, and InN.²¹ However, when comparing the absolute values of Δ_{so} with the results of future experiments, we have to take into consideration the fact that the mixing between the d -states of the cation and the p -states of N is strongly overestimated in the local density approximation, although we expect the trend is preserved.

Luttinger parameters in the $\mathbf{k} \cdot \mathbf{p}$ Hamiltonians are usually determined by fitting experimental data of valence-band spectra. Unfortunately, owing to long difficulty in growing high-quality crystals, no information is currently available from experiments in group-III nitrides. Then, first-principles

TABLE V. Fundamental band gap energies E_g and full valence bandwidths, ΔE_v (in eV) as obtained from FLAPW calculations for Si, BN, AlN, GaN, and InN. The results for nonrelativistic and full relativistic calculations are shown.

	Nonrelat.		Full relat.	
	E_g	ΔE_v	E_g	ΔE_v
Si	0.63	11.75	0.60	11.81
BN	4.47	20.08	4.45	20.11
AlN	3.31	14.83	3.31	14.87
GaN	1.72	15.57	1.53	15.69
InN	-0.11	15.22	-0.48	14.79

TABLE VI. Spin-orbit splitting energy Δ_{so} (in meV) for cubic Si, BN, AlN, GaN, and InN.

	Si	BN	AlN			GaN				InN			
Δ_{so}	44 ^a	47 ^g	21 ^g	19 ^{b,e}	20 ^d	19 ^g	15 ^b	17 ^{c,f}	20 ^d	19 ^e	13 ^g	6 ^b	3 ^g

^aReference 48—expt. value.^bReference 21—FLAPW method.^cReference 54—expt. value.^dReference 55—FLAPW method.^eReference 56—FLMTO method.^fReference 57—empirical pseudopotential method.^gThis work.

band-structure calculations can assist in determining these important parameters and in understanding the upper valence-band spectra of these materials. In order to calculate the Luttinger parameters for silicon and for the nitrides, we first provide values for effective masses, and from them we will derive Luttinger parameters.

III. DERIVATION OF EFFECTIVE-MASS PARAMETERS

A. Effective-mass approximation

The use of the effective-mass Hamiltonian for zinc-blende semiconductors will be briefly described in this section. This Hamiltonian depends on the approximations that are made to simplify its most general form. We adopt the effective-mass Hamiltonian derived by Luttinger-Kohn (LK) (Ref. 58) using the $\mathbf{k} \cdot \mathbf{p}$ method. In general, the linear terms with respect to wave vector \mathbf{k} that are nonzero in the presence of symmetry

inversion (case of Si) are neglected. Considering only the quadratic terms with respect to \mathbf{k} , we may construct the LK Hamiltonian for the top of the valence-band states. In the presence of the spin-orbit interaction, the Γ_{15} state is decomposed into the Γ_7 and Γ_8 states. We neglected the coupling between the conduction and valence-band states.

The eigenvalues of the (6×6) LK Hamiltonian are required as functions of wave-vector \mathbf{k} in parabolic approximation. Such calculations have been previously performed by us for GaAs (Ref. 59) and Si (Ref. 60). To derive these functions, the LK Hamiltonian must be specified. The total Hamiltonian is composed by the $\mathbf{k} \cdot \mathbf{p}$ part $H_{\mathbf{k} \cdot \mathbf{p}}$, and the spin-orbit interaction H_{so} . Using the states $|jm_j\rangle$ that correspond to the four Γ_8 heavy- and light-hole valence-band states $|\frac{3}{2}m_{3/2}\rangle$, with $m_{3/2} = \pm \frac{3}{2}, \pm \frac{1}{2}$, and the two Γ_7 split-off valence-band states $|\frac{1}{2}m_{1/2}\rangle$, with $m_{1/2} = \pm \frac{1}{2}$ the total Hamiltonian matrix $\langle jm_j|H_{\mathbf{k} \cdot \mathbf{p}}+H_{so}|j'm_j'\rangle$ is written as

$$\begin{vmatrix} Q & S & R & 0 & \frac{i}{\sqrt{2}}S & -i\sqrt{2}R \\ S^* & T & 0 & R & -\frac{i}{\sqrt{2}}(Q-T) & i\sqrt{\frac{3}{2}}S \\ R^* & 0 & T & -S & -i\sqrt{\frac{3}{2}}S^* & -\frac{i}{\sqrt{2}}(Q-T) \\ 0 & R^* & -S^* & Q & -i\sqrt{2}R^* & -\frac{i}{\sqrt{2}}S^* \\ -\frac{i}{\sqrt{2}}S^* & \frac{i}{\sqrt{2}}(Q-T) & i\sqrt{\frac{3}{2}}S & i\sqrt{2}R & \frac{1}{2}(Q+T)-\Delta_{so} & 0 \\ i\sqrt{2}R^* & -i\sqrt{\frac{3}{2}}S^* & \frac{i}{\sqrt{2}}(Q-T) & \frac{i}{\sqrt{2}}S & 0 & \frac{1}{2}(Q+T)-\Delta_{so} \end{vmatrix}, \quad (1)$$

where

$$Q = -\frac{\hbar^2}{2m}[(\gamma_1 + \gamma_2)(k_x^2 + k_y^2) + (\gamma_1 - 2\gamma_2)k_z^2],$$

$$T = -\frac{\hbar^2}{2m}[(\gamma_1 - \gamma_2)(k_x^2 + k_y^2) + (\gamma_1 + 2\gamma_2)k_z^2],$$

$$S = i\frac{\hbar^2}{m}\sqrt{3}\gamma_3(k_x - ik_y)k_z,$$

$$R = -\frac{\hbar^2}{2m}\sqrt{3}[\gamma_2(k_x^2 - k_y^2) - 2i\gamma_3k_xk_y], \quad (2)$$

TABLE VII. Effective masses for electrons (e), heavy-holes (hh), light-holes (lh) and spin-orbit split-holes (so) (in units of the free electron mass m) in (100), (110), and (111) directions for cubic Si, BN, AlN, and GaN.

Ref.	m_e	$m_{hh}^{(100)}$	$m_{lh}^{(100)}$	$m_{hh}^{(111)}$	$m_{lh}^{(111)}$	$m_{hh}^{(110)}$	$m_{lh}^{(110)}$	m_{so}
Si								
This work	0.96 (m_I), g 0.92 (m_I), h i	0.16 (m_t), 0.19 (m_t)	0.26	0.18	0.67	0.13	0.54	0.14 0.22 0.23
			0.46	0.17	0.56	0.16	0.53	0.16
			0.43	0.19	0.27		0.43	0.24
BN								
This work	0.94 (m_I), ALN	0.23 (m_t)	0.53	0.51	1.26	0.33	1.09	0.35 0.51
a	0.21 (Γ), 0.53 (m_I), c 0.30 (Γ)	0.31 (m_t)	1.02	0.35	2.85	0.30	2.16	0.31 0.51
e	0.19 (Γ)		1.39	0.44				
This work	0.28 (Γ), 0.53 (m_I), 1.95 (m_t)		1.44	0.42	4.24	0.36	3.03	0.37 0.63
GaN								
a	0.13		0.74	0.21	1.82	0.18	1.51	0.19 0.33
b	0.20		0.42	0.20				
c	0.17		0.85	0.24				
d	0.16		0.87		1.95	0.18	0.84	0.19
e	0.11		0.80	0.18	2.40			0.26
f	0.15							
This work	0.14		0.86	0.21	2.09	0.19	1.65	0.19 0.30

^aEmpirical pseudopotential calculations from Ref. 17.

^b $\mathbf{k} \cdot \mathbf{p}$ calculations from Ref. 61—obtained from γ_i parameters.

^cFLAPW calculations from Ref. 55—obtained from γ_i parameters.

^dFLAPW method without spin-orbit interaction from Ref. 20.

^eEmpirical pseudopotential calculations from Ref. 23.

^fExpt. value from Ref. 62.

^gReference 48—expt. values.

^hReference 64—expt. values.

ⁱReference 65—expt. values.

m is the free electron mass, and γ_1 , γ_2 , and γ_3 are the (dimensionless) Luttinger parameters.

B. Effective masses and Luttinger parameters

As we are interested in obtaining the conduction- and valence-band effective masses, we focus our attention on the electronic structure around the valence-band maximum and the conduction-band minimum at the center of the BZ, and we will link these band structures with the effective-mass theory. We calculated heavy-hole (m_{ph}), light-hole (m_{lh}), and split-off-hole (m_{so}) effective masses in (100), (110), and (111) directions, and the electron effective mass. In order to calculate the conduction-band effective masses, we adopted a parabolic band model at the Γ point for GaN, at the X point for BN and AlN, and at the intermediate point of the Γ - X line for Si. Since a negative value for the InN band gap is obtained from the *ab initio* FLAPW calculations within LDF theory, it was not possible to derive reliable values for its effective masses.

For BN, AlN, and Si we calculated the transverse (m_t) and longitudinal (m_l) electron masses at the conduction-band minimum. The isotropic electron effective mass at Γ has been calculated for GaN. Although our FLAPW calculations show that AlN is an indirect-gap material, we also calculated the isotropic electron effective mass at Γ since it is controversial whether AlN is a direct- or an indirect-gap material.^{35,36} The hole effective masses were obtained by fit-

TABLE VIII. Luttinger parameters γ_1 , γ_2 , and γ_3 for Si.

Ref.	66 ^a	67	68 ^b	This work
γ_1	4.27	4.22	4.61	4.65
γ_2	0.32	0.39	0.39	0.44
γ_3	1.46	1.44	1.54	1.57

^aObtained from A, B, and N parameters according to the relations in Ref. 51.

^bObtained from A, B, and C parameters according to the relations in Ref. 51.

TABLE IX. Luttinger parameters γ_1 , γ_2 , and γ_3 for cubic BN, AlN, and GaN.

BN			AlN			GaN			
Ref.	This work	55	63 ^b	This work	17 ^a	55	61	63 ^b	This work
γ_1	1.92	1.50	1.81	1.54	3.06	2.70	3.75	3.16	2.96
γ_2	0.02	0.39	0.50	0.42	0.85	0.76	0.69	1.21	0.90
γ_3	0.56	0.62	0.88	0.64	1.25	1.07	1.44	1.51	1.20

^aExtracted from the masses according to expressions (3).

^bDirect calculation from semiempirical eigenfunctions.

ting to a parabola the curves of energy versus \mathbf{k} taken from Γ up to 0.5% along the ΓK , ΓX , and ΓL lines. The electron effective masses were obtained in a similar way by calculating the energy curves starting from the conduction-band minimum at Γ , X , or at the intermediate point (Si).

Effective-mass values are listed in Table VII for Si, BN, AlN, and GaN. Since the effective mass of the split-off band does not show any relevant dependence on \mathbf{k} direction, the values depicted in Table VII for m_{so} are the isotropic ones.

In order to obtain the expressions that relate the Luttinger parameters to the effective masses for holes, we have to diagonalize the LK matrix (1) and evaluate its six eigenvalues. There are three twofold spin-degenerate bands, the heavy-hole (hh), light-hole (lh) and spin-orbit split-off-hole (so) bands. Fixing a certain wave-vector \mathbf{k} and neglecting nonparabolic terms in \mathbf{k} , the effective masses for the highest-symmetry directions may be defined in terms of the Luttinger parameters.^{51,60} One obtains

$$\begin{aligned}\gamma_1 &= \frac{1}{2} [m_{lh}^{-1}(100) + m_{hh}^{-1}(100)], \\ \gamma_2 &= \frac{1}{4} [m_{lh}^{-1}(100) - m_{hh}^{-1}(100)] \\ \gamma_3 &= \frac{1}{4} [m_{lh}^{-1}(111) - m_{hh}^{-1}(111)].\end{aligned}\quad (3)$$

By using the above equations and the obtained values for the effective masses, we evaluated the Luttinger parameters, γ_i , which are shown in Table VIII for Si.

The four parameters Δ_{so} , γ_1 , γ_2 , and γ_3 of the six-band LK model are very important for calculations of other systems, such as quantum wells and superlattices that need these parameters as inputs. While the spin-orbit splitting energy for Si is well-known $\Delta_{so}=44$ meV⁴⁸ there is a considerable number of different sets of Luttinger parameters in the literature. In Table VIII we show some of them. One notices that,

despite few discrepancies, our values are in excellent agreement with the experimental data reported in Ref. 66 and with previous calculations.^{67,68} Table IX depicts the Luttinger parameters for cubic BN, AlN, and GaN. As we may observe, there are discrepancies between the different sets of parameters obtained by several authors. Particularly for GaN, which is by far the most studied nitride, our values for the γ_i parameters compare fairly well with those obtained from other first-principles calculations.

IV. CONCLUSION

In this paper, we have presented structural and electronic properties of the III-N semiconductor compounds BN, AlN, GaN, and InN, in the cubic phases, and of Silicon as obtained through first-principles calculations using the FLAPW method within the LDF-GGA approximation. The calculated equilibrium lattice constants, bulk moduli, cohesive energies, and spin-orbit splitting energies were compared with those obtained through other methods and with experimental values when available, and showed very good agreement. Band-structure derived effective masses are provided for all materials, except InN, for reasons discussed. From the effective masses, we evaluated the Luttinger parameters, γ_1 , γ_2 , and γ_3 , thus providing sets of such parameters for the group-III nitrides. The corresponding calculations performed for Si, for which there are several theoretical and experimental results, reveal excellent accordance, reinforcing the accuracy of the results obtained for the nitrides. The present results will be relevant and useful for theoretical investigations on quantum wells and superlattices derived from group-III nitrides, which use the Luttinger-Kohn theory coupled with the $\mathbf{k} \cdot \mathbf{p}$ method.

ACKNOWLEDGMENTS

The authors would like to thank FAPESP and CNPq (Brazilian funding agencies) for partial financial support.

¹S. Nakamura, *Semicond. Sci. Technol.* **14**, R27 (1999).

²S. Nakamura and G. Fasol, *The Blue Laser Diode* (Springer, Berlin, 1997).

³For recent reviews see, e.g., J.W. Orton, and C.T. Foxon, *Rep. Prog. Phys.* **61**, 1 (1998); in *Gallium Nitride I*, in *Semicond.*

Semimet. Vol. 50, edited by J. I. Pankove and T. D. Moustakas (Academic, London, 1998).

⁴*Properties of Group-III Nitrides*, edited by J.H. Edgar (INSPEC, London, 1994).

⁵S. Okubo, N. Shibata, T. Saito, and Y. Ikuhara, *J. Cryst. Growth*

- ¹⁹⁰ 452 (1998).
- ⁶ M.J. Paisley, Z. Sitar, J.B. Posthill, and R.F. Davis, *J. Vac. Sci. Technol. A* **7**, 701 (1989).
- ⁷ Z. Sitar, M.J. Paisley, J. Ruan, J.W. Choyke, and R.F. Davis, *J. Mater. Sci. Lett.* **11**, 261 (1992).
- ⁸ T.S. Cheng, L.C. Jenkins, S.E. Hooper, C.T. Foxon, J.W. Orton, and D.E. Lacklison, *Appl. Phys. Lett.* **66**, 1509 (1995).
- ⁹ D. Schikora, M. Hankeln, D.J. As, K. Lischka, T. Litz, A. Waag, T. Buhrow, and F. Henneberger, *Phys. Rev. B* **54**, R8381 (1996).
- ¹⁰ A. Tabata, R. Enderlein, J.R. Leite, S.W. da Silva, J.C. Galzerani, D. Schikora, M. Kloiddt, and K. Lischka, *J. Appl. Phys.* **79**, 4137 (1996).
- ¹¹ A. Tabata, A.P. Lima, L.K. Teles, L.M.R. Scolfaro, J.R. Leite, V. Lemos, B. Schöttker, T. Frey, D. Schikora, and K. Lischka, *Appl. Phys. Lett.* **74**, 362 (1999); A.P. Lima, A. Tabata, J.R. Leite, S. Kaiser, D. Schikora, B. Schöttker, T. Frey, D.J. As, and K. Lischka, *J. Cryst. Growth* **202**, 396 (1999).
- ¹² A. Tabata, J.R. Leite, A.P. Lima, E. Silveira, V. Lemos, T. Frey, D.J. As, D. Schikora, and K. Lischka, *Appl. Phys. Lett.* **75**, 1095 (1999); V. Lemos, E. Silveira, J.R. Leite, A. Tabata, R. Trentin, L.M.R. Scolfaro, T. Frey, D.J. As, D. Schikora, and K. Lischka, *Phys. Rev. Lett.* **84**, 3666 (2000).
- ¹³ H. Harima, T. Inoue, S. Nakashima, H. Okumura, Y. Ishida, S. Yoshida, T. Koizumi, H. Grille, and F. Bechstedt, *Appl. Phys. Lett.* **74**, 191 (1999).
- ¹⁴ W.E. Pickett, *Phys. Rev. B* **38**, 1316 (1988).
- ¹⁵ V.K. Gupta, C.C. Wamsley, M.W. Koch, and G.W. Wicks, *J. Vac. Sci. Technol. B* **17**, 1246 (1999).
- ¹⁶ S.C.P. Rodrigues, L.M.R. Scolfaro, J.R. Leite, and G.M. Sipahi, *Appl. Phys. Lett.* **76**, 1015 (2000).
- ¹⁷ W.J. Fan, M.F. Li, T.C. Chong, and J.B. Xia, *J. Appl. Phys.* **79**, 188 (1996).
- ¹⁸ Y.C. Yeo, T.C. Chong, and M.F. Li, *J. Appl. Phys.* **83**, 1429 (1998).
- ¹⁹ M. Suzuki, T. Uenoyama, and A. Yanase, *Phys. Rev. B* **52**, 8132 (1995).
- ²⁰ J.L.A. Alves, H.W.L. Alves, C. de Oliveira, R.D.S.C. Valadão, and J.R. Leite, *Mater. Sci. Eng. B* **50**, 57 (1997).
- ²¹ S.-H. Wei and A. Zunger, *Appl. Phys. Lett.* **69**, 2719 (1996).
- ²² C. Stampfli and C.G. Van de Walle, *Phys. Rev. B* **59**, 5521 (1999).
- ²³ S.K. Pugh, D.J. Dugdale, S. Brand, and R.A. Abram, *Semicond. Sci. Technol.* **14**, 23 (1999).
- ²⁴ D.J. Dugdale, S. Brand, and R.A. Abram, *Phys. Rev. B* **61**, 12 933 (2000).
- ²⁵ For a detailed discussion on effective-mass parameters, see for example, R. Enderlein, G.M. Sipahi, L.M.R. Scolfaro, and J.R. Leite, *Phys. Status Solidi B* **206**, 623 (1998).
- ²⁶ P. Blaha, K. Schwarz, and J. Luitz, WIEN97, *A Full Potential Linearized Augmented Plane-Wave Package for Calculating Crystal Properties*, edited by Karlheinz Schwarz (Techn. Univ. Wien, Vienna, 1999) ISBN Report No. 3-9501031-0-4. Updated version of P. Blaha, K. Schwarz, P. Sorantin, and S.B. Trickey, *Comput. Phys. Commun.* **59**, 399 (1990).
- ²⁷ K. Schwarz and P. Blaha, *Lect. Notes Chem.* **67**, 139 (1996).
- ²⁸ J.P. Perdew, K. Burke, and M. Ernzerhof, *Phys. Rev. Lett.* **77**, 3865 (1996).
- ²⁹ D.D. Koelling and B.N. Harmon, *J. Phys. C* **10**, 3107 (1977).
- ³⁰ P. Novák (unpublished). Distributed with the WIEN97 FLAPW package.
- ³¹ F.D. Murnaghan, *Proc. Natl. Acad. Sci. U.S.A.* **30**, 244 (1944).
- ³² D.J. Singh, *Plane Waves, Pseudopotentials and the LAPW Method* (Kluwer Academic Publishers, Boston, 1994).
- ³³ J.P. Desclaux, *Comput. Phys. Commun.* **1**, 216 (1969); **9**, 31 (1975).
- ³⁴ V. Fiorentini, M. Methfessel, and M. Scheffler, *Phys. Rev. B* **47**, 13 353 (1993).
- ³⁵ T. Lei, T.D. Moustakas, R.J. Graham, Y. He, and S.J. Berkowitz, *J. Appl. Phys.* **71**, 4933 (1992).
- ³⁶ I. Petrov, E. Mojab, R.C. Powell, J.E. Greene, L. Hultman, and J.-E. Sundgren, *Appl. Phys. Lett.* **60**, 2491 (1992).
- ³⁷ S. Strite, D. Chandrasekhar, D.J. Smith, J. Sariel, H. Chen, N. Teraguchi, and H. Morkoç, *J. Cryst. Growth* **127**, 204 (1993).
- ³⁸ K. Kim, W.R.L. Lambrecht, and B. Segall, *Phys. Rev. B* **53**, 16 310 (1996).
- ³⁹ Y.-N. Xu and W.Y. Ching, *Phys. Rev. B* **44**, 7787 (1991).
- ⁴⁰ N.E. Christensen and I. Gorczyca, *Phys. Rev. B* **50**, 4397 (1994).
- ⁴¹ A.F. Wright and J.S. Nelson, *Phys. Rev. B* **50**, 2159 (1994); **51**, 7866 (1995).
- ⁴² M. van Schilfgaarde, A. Sher, and A.-B. Chen, *J. Cryst. Growth* **178**, 8 (1997).
- ⁴³ M. Ueno, M. Yoshida, A. Onodera, O. Shimomura, and K. Takeamura, *Phys. Rev. B* **49**, 14 (1994); M. Ueno, A. Onodera, O. Shimomura, and K. Takemura, *ibid.* **45**, 10 123 (1992).
- ⁴⁴ B. Paulus, E.-J. Shi, and H. Stoll, *J. Phys.: Condens. Matter* **9**, 2745 (1997).
- ⁴⁵ W.A. Harrison, *Electronic Structure and the Properties of Solids* (Dover, New York, 1989).
- ⁴⁶ M. Palummo, L. Reining, R.W. Godby, C.M. Bertoni, and N. Börnsen, *Europhys. Lett.* **26**, 607 (1994).
- ⁴⁷ R.M. Wentzcovitch, K.J. Chang, and M.L. Cohen, *Phys. Rev. B* **34**, 1071 (1986).
- ⁴⁸ G. Harbecke, O. Madelung, and U. Rössler, in *Numerical Data and Functional Relationships in Science and Technology*, edited by O. Madelung, Landolt-Börnstein, New Series, Group III, Vol. 17 (Springer-Verlag, Berlin, 1982).
- ⁴⁹ C. Persson and E. Janzen, *J. Phys.: Condens. Matter* **10**, 10 549 (1998).
- ⁵⁰ M. Städele, M. Moukara, J.A. Majewski, P. Vogl, and A. Görling, *Phys. Rev. B* **59**, 10 031 (1999).
- ⁵¹ R. Enderlein and N.J.M. Horing, *Fundamentals of Semiconductor Physics and Devices* (World Scientific, Singapore, 1997).
- ⁵² D. Vogel, P. Krüger, and J. Pollmann, *Phys. Rev. B* **55**, 12 836 (1997).
- ⁵³ M. Städele, J.A. Majewski, P. Vogl, and A. Görling, *Phys. Rev. Lett.* **79**, 2089 (1997).
- ⁵⁴ G. Ramírez-Flores, H. Navarro-Contreras, A. Lastras-Martínez, R.C. Powell, and J.E. Greene, *Phys. Rev. B* **50**, 8433 (1994).
- ⁵⁵ M. Suzuki and T. Uenoyama, *Appl. Phys. Lett.* **69**, 3378 (1996).
- ⁵⁶ K. Kim, W.R.L. Lambrecht, B. Segall, and M. van Schilfgaarde, *Phys. Rev. B* **56**, 7363 (1997).
- ⁵⁷ A. Tadjer, B. Abbar, M. Rezki, H. Aourag, and M. Certier, *J. Phys. Chem. Solids* **60**, 419 (1999).
- ⁵⁸ J.M. Luttinger and W. Kohn, *Phys. Rev.* **97**, 869 (1955).
- ⁵⁹ G.M. Sipahi, R. Enderlein, L.M.R. Scolfaro, and J.R. Leite, *Phys. Rev. B* **53**, 9930 (1996).
- ⁶⁰ A.L. Rosa, L.M.R. Scolfaro, R. Enderlein, G.M. Sipahi, and J.R.

- Leite, Phys. Rev. B **58**, 15 675 (1998).
⁶¹D. Ahn, J. Appl. Phys. **79**, 7731 (1996).
⁶²M. Fanciulli, T. Lei, and T.D. Moustakas, Phys. Rev. B **48**, 15 144 (1993).
⁶³S.K. Pugh, D.J. Dugdale, R.A. Coles, S. Brand, and R.A. Abram, in *Proceedings of the 24th International Conference on the Physics of Semiconductor*, edited by D. Gershoni, CD-Rom (World Scientific, Jerusalem, Israel, 1998).
⁶⁴R.N. Dexter and B. Lax, Phys. Rev. **96**, 223 (1954).
⁶⁵R.N. Dexter, H.J. Zeiger, and B. Lax, Phys. Rev. **104**, 637 (1956).
⁶⁶I. Balslev and P. Lawaetz, Phys. Lett. **19**, 6 (1965).
⁶⁷P. Lawaetz, Phys. Rev. B **4**, 3460 (1971).
⁶⁸C. Persson and U. Lindefelt, Phys. Rev. B **54**, 10 257 (1996).